Developmental Dynamics

Knockdown of Slit signalling during limb development leads to a reduction in humerus length

Journal:	*Developmental Dynamics*
Manuscript ID	LDDVDY-20-0085.R2
Wiley - Manuscript type:	Patterns & Phenotypes
Date Submitted by the Author:	n/a
Complete List of Authors:	Rafipay, Alexandra; University of Aberdeen, School of Medicine, Medical Sciences & Nutrition Dun, Xin-Peng; University of Plymouth, Peninsula School of Medicine and Dentistry Parkinson, David; University of Plymouth, Peninsula School of Medicine and Dentistry Erskine, Lynda; University of Aberdeen, School of Medicine, Medical Sciences and Nutrition Vargesson, Neil; University of Aberdeen, School of Medicine, Medical Sciences and Nutrition
Keywords:	Robo, Forelimb, Hindlimb, Gene expression, Bone development, Slit, Mouse, Chicken, Mouse mutant, Dominant-negative

Knockdown of Slit signalling during limb development leads to a reduction in humerus length

Alexandra Rafipay[1], Xin-Peng Dun[2], David B Parkinson[2], Lynda Erskine[1], Neil Vargesson[1*]

[1] Institute of Medical Sciences, School of Medicine, Medical Sciences and Nutrition, University of Aberdeen, Foresterhill, Aberdeen, AB25 2ZD

[2] Peninsula Medical School, Faculty of Health, University of Plymouth, Plymouth, PL6 8BU, United Kingdom

Keywords: Robo; Slit; Mouse; Mouse knockout; Chicken; Forelimb; Hindlimb; Gene expression; Bone development.

Grant Sponsor and Number: EastBio DTP PhD studentship to AR

***Author for Correspondence:**
Professor Neil Vargesson
Institute of Medical Sciences
School of Medicine, Medical Sciences and Nutrition
University of Aberdeen
Foresterhill
Aberdeen
AB25 2ZD
n.vargesson@abdn.ac.uk
+44 (0)1224 437374

Abstract

Background: Slits (1-3) and their Robo (1-3) receptors play multiple non-neuronal roles in development, including in development of muscle, heart and mammary gland. Previous work has demonstrated expression of *Slit* and *Robo* family members during limb development, where their functions are unclear. Results: *In situ* hybridisation confirmed strong expression of *Slit2, Slit3*, *Robo1,* and *Robo2* throughout mouse limb and joint development. No expression of *Slit1* or *Robo3* was detected. Analysis of *Slit1/2* or *Slit3* knockout mice revealed normal limb development. In contrast, locally blocking Slit signalling though grafting of cells expressing a dominant-negative *Robo2* construct in the proximo-central region of developing chicken limb buds caused significant shortening of the humerus. Conclusions: These findings demonstrate an essential role for Slit/Robo signalling in regulating bone length during chicken limb development.

Introduction

Secreted Slit ligands bind to Roundabout (Robo) receptors to initiate cell signalling identified initially for its role in regulating axon guidance. Since their discovery in *Drosophila*, four *Robo* (Robo 1-4) and three *Slit* (Slit 1-3) homologs have been identified in vertebrates, although *Robo4* is only expressed in endothelial cells.[1-9] As well as guiding axons at multiple regions in the developing nervous system,[10] Slit/Robo signalling also has non-neuronal roles including in development of lung,[11] kidney and mammary gland.[12-15] Additionally, Slit/Robo signalling can promote and inhibit endothelial cell migration and angiogenesis,[16-19] and is required during heart development with *Robo1/2* mutant mice presenting with partial absence of pericardium, reduced sinus horn myocardium and alignment defects of caval veins.[20] In *Drosophila*, *Slit* acts as a long range chemorepellent to drive the migration of muscle precursor cells away from the midline,[5] and expression of *Slit* at epidermal muscle attachment sites arrests migration of muscle cells to facilitate correct development of muscle-tendon attachment sites.[21-24]

Reflecting their roles during development of multiple tissues, *Slits* and *Robos* are expressed in regions of the developing vertebrate embryo outside the nervous system such as branchial arches, reproductive organs, developing heart and kidney and the limb bud of mouse and chicken embryos, particularly in and around the forming joints and muscle regions.[2,6,9,11,18,25-27] Here we focus on the nature and role of *Slit/Robo* signalling during limb development.

Expression of *Slits* and *Robos* has been reported in developing mouse and chicken limbs, and are grossly comparable.[2,9,26,27] However, there is a disparity in the reported expression of *Slit1* in the developing mouse limb. No expression of *Slit1* was described during mouse limb development by Yuan et al. 1999[9] but was described at E12.5 in posterior and anterior margins and at the digit tips and over the joints at E13.5 by Holmes et al. 1998.[2] Published expression patterns suggest multiple potential roles for Slit-Robo signalling during limb development. For example, central mesenchyme expression patterns of *Robos* are similar to those of muscle markers[27], and *Slits* are expressed in domains of migrating myoblasts,[26,27] though no expression of *Slits* or *Robos* co-localises with differentiating myoblasts.[27] Expression of *Slits* and *Robos* also are detected interdigitally, along digit borders in patterns resembling developing tendons, and in presumptive joint sites.[2,9,26,27] Axon guidance pathways also have been linked to bone development and human joint disorders, and fibroblasts within joints of patients with rheumatoid arthritis show increased *Robo3* and decreased *Slit3* expression.[28] However, despite analysis of limb expression patterns, the precise roles of Slit/Robo signalling during vertebrate limb development remains unknown.

In this paper, we have analysed *Slit* and *Robo* expression patterns in mouse fore- and hind-limbs and confirm that *Slit1* is not expressed in the developing mouse limb. We utilise *Slit* knockout mice[29,30] to show that knockdown of individual *Slit* genes or *Slit1* and *Slit2* in combination does not impact upon mouse limb development. Limb length and expression patterns of markers for joint, muscle, blood vessel, tendon and nerve development are normal. In contrast, locally inhibiting Slit signalling in the proximo-central region of developing chicken limb buds resulted in a shortening of

the length of the humerus. These findings demonstrate that Slit signalling has an essential role in controlling the length of limb elements.

Results

Slit and *Robo* expression patterns support a role for Slit-Robo signalling in mouse limb and joint development

To confirm which specific *Slit* and *Robo* family members are expressed in developing mouse limbs, and the temporo-spatial patterns of their expression, we used whole mount *in situ* hybridisation with mRNA riboprobes against *Slit1, Slit2, Slit3* and *Robo1*, *Robo2* and *Robo3*. Analyses were carried out at E13.5 (the point at which digits become discernible, nerves have entered the hand- and foot-plate and development of muscles starts to be seen), through to E15.5 (distal phalanges have formed, digits have separated and the nerve plexus has reached the fingertips).[31,32] Earlier expression patterns have been mapped in detail previously,[2,9,27] although apparently disparate patterns for *Slit1* and *Slit3* have been reported.[2,9]

In agreement with Yuan et al 1999[9], no *Slit1* expression was detected in the fore- and hindlimb between E13.5 and E15.5 in whole mount and section images (Figure 1a, a', g, g', m, m', s). In contrast, strong expression of both *Slit2* (Figure 1b, b', h, h', n, n', t) and *Slit3* (Figure 1c, c', i, I', o, o', u) were detected in both the developing fore- and hind-limbs. In both the fore- and hindlimbs, *Slit2* was expressed in the interdigital regions and digit borders at E13.5 through to E14.5, with strongest expression at E13.5 (Figure 1b, b' arrowheads). At E14.5 and E15.5, expression of *Slit2* was restricted to the digit borders visible in whole mount and section images (Figure 1h, h' n, n', t arrowhead). In contrast to *Slit2*, expression of *Slit3* intensified through development from E13.5 to E15.5 and was seen in proximal fore- and hind-limb mesenchyme at E13.5 (Figure 1c, c'). At E14.5 and E15.5 *Slit3* was expressed along proximal digit borders, with broader regions of expression just proximal to

presumptive joint regions (Figure 1i, i', o, o' arrows), with a weak expression band visible at the distal interphalangeal joint of E15.5 limbs (Figure 1o, o' arrowheads). Sections through the digits demonstrated strong expression of *Slit3* surrounding the digits as well as in mesenchyme ventral to the digits (Figure 1u).

At E13.5, *Robo1* was expressed in the hand- and foot-plate, as well as at the metacarpophalangeal/metatarsophalangeal joints (Figure 1d, d' arrowheads). A low level of expression was observed at the proximal interphalangeal joint in the E13.5 forelimb (Figure 1d arrow), however no expression was visible at the proximal interphalangeal joint in the E13.5 hindlimb (Figure 1d'). At E14.5 *Robo1* was expressed in both the hand- and foot-plate, and in the proximal and distal interphalangeal joints (Figure 1j, j'). By E15.5 expression was clearly visible in the metacarpophalangeal/metatarsophalangeal and interphalangeal joints (Figure 1p, p' arrowhead). Sections through the interphalangeal joints at E15.5 demonstrated *Robo1* expression around the periphery of the joints (Figure 1v). *Robo2* was expressed in the forming cartilage condensations of E13.5 forelimb handplates (Figure 1e). In contrast *Robo2* expression in the hindlimb was restricted mainly to the footplate with small regions of expression visible in interdigital regions around digits 1 and 5 (Figure 1e' arrowhead). At E14.5 *Robo2* was visible at the site of the proximal interphalangeal joint. and at the metacarpophalangeal/metatarsophalangeal joints (Figure 1k, k'). By E15.5 *Robo2* was expressed at the distal interphalangeal joint as observed in whole mount and section images (Figure 1q, q', w arrowheads). *Robo2* was expressed at the borders of the metacarpophalangeal/metatarsophalangeal joints (Figure 1q, q', w arrows). At all ages examined *Robo3* was not expressed in the developing mouse limb, confirming previous observations (Figure 1f, f', l, l', r, r', x).[27]

Loss of Slit1 and Slit2 does not affect mouse limb development

Slits and Robos have been linked to joint disorders such as scoliosis, kyphosis and arthritis.[28,33,34] To investigate if Slit/Robo signalling is essential for normal joint development and maintenance, we analysed fore- and hind-limbs from *Slit1*$^{-/-}$ *Slit2*$^{-/-}$ mouse mutants[30] and control (*Slit1*$^{-/-}$ *Slit2*$^{+/+}$ littermates or wild-type) embryos using markers for joint (*Gdf5*), connective tissue (*Scx*), muscle (*Myod1*), blood vessel (*Cdh5*) and neuronal development (anti-neurofilament antibody).[32] Because Slit1 and Slit2 can function redundantly[30] and it is potentially possible that our expression analyses may have failed to detect very low levels of *Slit1* in the developing limbs, *Slit2*$^{-/-}$ mice were analysed on a *Slit1*$^{-/-}$ background, by breeding *Slit1*$^{-/-}$ *Slit2*$^{+/-}$ mice. We also analysed crosses of *Slit1*$^{+/-}$ mice to confirm loss of *Slit1* alone had no impact on limb development.

As expected, since no expression of *Slit1* was observed in developing limbs, *Slit1*$^{-/-}$ fore- and hindlimbs appeared phenotypically normal (Figure 1a, g, m; Figure 2A, B, C). Fore- and hindlimbs of *Slit1*$^{-/-}$ *Slit2*$^{-/-}$ mutants also appeared grossly normal and there were no significant differences in the relative length of the forelimbs or hindlimbs of *Slit1*$^{-/-}$ mutants or *Slit1*$^{-/-}$ *Slit2*$^{-/-}$ mutants compared to littermate controls (*Slit1*$^{+/+}$ or *Slit1*$^{-/-}$ *Slit2*$^{+/+}$ respectively; Figure 2A, B). Development of joints, connective tissue, muscle, blood vessels and nerves also appeared similar between wild-type (*Slit1*$^{+/+}$) and *Slit1*$^{-/-}$ *Slit2*$^{-/-}$ limbs. At E15.5 *Gdf5*, a marker of joint development, was expressed in carpometacarpal, metacarpophalangeal, proximal (Figure 2C white arrows) and distal interphalangeal joints in wild-type and *Slit1*$^{-/-}$ *Slit2*$^{-/-}$ forelimbs (Figure 2C). Expression of *Cdh5*, an endothelial cell marker, was observed throughout the upper and lower limb mesenchyme and in the hand-plate up to the proximal interphalangeal joint along the digits in wild-type and *Slit1*$^{-/-}$ *Slit2*$^{-/-}$ limbs. More intense regions of *Cdh5* expression were seen interdigitally, at the digit base (Figure 2C black arrows) and avascular regions were normally visible at the digit tips in all genotypes analysed. No obvious differences in expression patterns of *Cdh5* were observed between wild type and mutant mice (Figure 2C). At E14.5 expression of *Scx (Scleraxis)*, a marker of developing tendons, was observed as distinct bands of expression in wild-type and *Slit1*$^{-/-}$ *Slit2*$^{-/-}$ limbs extending along digits from the foot-plate, with expression also seen at developing joint sites (Figure 2C black arrowheads). At E15.5 *Myod1,*

which is expressed in muscle fibres, was expressed in the upper limb and in the footplate proximal to the digits in both wild type and *Slit1*$^{-/-}$*Slit2*$^{-/-}$ hindlimbs (Figure 2C).

At E11.5, the patterning of main nerve branches entering the forelimb and hindlimb also were not different between *Slit1*$^{+/+}$, *Slit1*$^{-/-}$ and *Slit1*$^{-/-}$ *Slit2*$^{-/-}$ mice (Figure 3a-c arrows, 3a'-c', asterisks). Nerves had progressed along the forelimb and entered the handplate by E13.5 (Figure 3d-f) and progressed to digit tips by E14.5, with no difference in nerve patterning between *Slit1*$^{+/+}$, *Slit1*$^{-/-}$ and *Slit1*$^{-/-}$ *Slit2*$^{-/-}$ mice (Figure 3g-i, arrowheads). These findings indicate that at the time points examined early neural patterning appears normal in *Slit1*$^{-/-}$ and *Slit1*$^{-/-}$ *Slit2*$^{-/-}$ mutant mouse limbs. Altogether, these data indicate phenotypically normal limbs in the absence of *Slit1* and *Slit2*.

Development of *Slit3* mutant mouse limbs also appeared phenotypically normal

Strong *Slit3* expression is seen during mouse limb development, we therefore sought to analyse *Slit3*$^{-/-}$ mouse limbs during development. A comparison of limb size along with whole mount in situ hybridisation analysis of *CdhH5* and *Myod1* in *Slit3*$^{-/-}$ limbs did not reveal any phenotypic difference between wild type and mutant limbs. There was no difference in limb length between *Slit3*$^{+/+}$ and *Slit3*$^{-/-}$ mice (Figure 4A). At E15.5, in both *Slit3*$^{+/+}$ and *Slit3*$^{-/-}$ forelimbs, C*dh5* was expressed through the handplate with strong expression along the digit borders (Figure 4B). *Myod1* was expressed in the proximal limb mesenchyme and in the handplate, with a central band of expression connecting expression regions of the proximal limb and handplate of *Slit3*$^{+/+}$ and *Slit3*$^{-/-}$ limbs (Figure 4B).

Robo2-Fc inhibits Slit-signalling

The lack of a mutant phenotype in *Slit1*$^{-/-}$*Slit2*$^{-/-}$ or *Slit3*$^{-/-}$ limbs raised the possibility that *Slit2* and *Slit3* might function redundantly during limb development. In support of this idea, previous

studies have demonstrated that multiple *Slit* alleles are often required to be lost before a phenotype is seen.[20,30,35-37] Moreover, in contrast to *Slit1*$^{-/-}$ mice which are viable and fertile, *Slit2*$^{-/-}$ pups die perinatally[30], as do more than 50% of *Slit3*$^{-/-}$ mutants.[38] Generation of *Slit2*$^{-/-}$ *Slit3*$^{-/-}$ embryos therefore would require breeding of *Slit2*$^{+/-}$ *Slit3*$^{+/-}$ mice meaning approximately only 1 in 16 embryos would be double mutants. We therefore sought an alternative approach for knocking down Slit2 and Slit3 signalling in the developing limb.

The ectodomain of Robo2 fused to the Fc domain of human immunoglobulin (Robo2-Fc) forms a soluble inhibitor of Slit activity that binds with high affinity to Slits but, because it lacks the intracellular domain, cannot mediate Slit signalling.[1,39] Robo2-Fc and Robo ectodomains fused to hemagglutinin have been used previously to attenuate the Slit-dependent growth and branching of cortical neurons and the inhibitory effect of the septum on migration of subventricular zone neurons.[39,40] To confirm that Robo2-Fc can attenuate Slit signalling in our hands we cultured E14.5 mouse retinal explants in collagen gels at a short distance (100 – 300 µm) from clusters of approximately 500 293T cells transfected with the vector alone or formed from a 1:1 mixture of control cells and cells transfected with *Robo2-Fc*, control cells and *Slit2*-transfected cells or *Robo2-Fc*- and *Slit2*-transfected cells (Figure 5A). Slit2 is a potent inhibitor of retinal ganglion cell axon outgrowth, decreasing the number and length of axons that extend from the retinal explants (Fig 5A, C).[41] Robo2-Fc alone had no effect on retinal ganglion cell axon outgrowth but attenuated the inhibitory effect of Slit2 (Figure 5 A, C). To confirm that Robo2-Fc can inhibit endogenous sources of Slit we co-cultured E14.5 mouse retina explants in collagen gels with tissue dissected from the ventral midline of the diencephalon. *Slit1* and *Slit2* are strongly expressed in the ventral diencephalon[41,42] and, in vitro, ventral diencephalon tissue secretes signals that are inhibitory to retinal ganglion cell axon outgrowth.[43] Seeding the collagen gel with *Robo2*-Fc transfected cells had no effect on the extent of retinal ganglion cell axon outgrowth compared to explants cultured in the presence of control cells (Figure 5B, D), but abrogated the inhibitory effect of ventral diencephalon tissue on axon outgrowth (Figure 5B, D). These findings confirm that Robo2-Fc can be used to inhibit slit signalling.

Local inhibition of Slit signalling by implanting *Robo2-Fc* transfected cells into the proximo-central region of early chicken embryo forelimb buds decreases the length of the humerus.

To investigate the effect of knocking down Slit signalling in the developing limb, we turned to the chicken embryo where we were able to locally inhibit signalling by all Slits by transplanting cells expressing *Robo2-Fc* into the proximo-central region of the forelimb bud, an area which fate map studies have demonstrated contributes to the humerus.[44] Comparison of *Slit* and *Robo* expression in developing mouse and chicken limbs demonstrated grossly similar patterns of expression.[2,9,26,27] However, in contrast to mouse, *SLIT1*, *SLIT2* and *SLIT3* are all expressed in the developing chicken limb (Table 1).[26,27] Aggregates of approximately 500 293T cells were grafted into the proximo-central region of HH St21 (E3.5) chicken limbs. To confirm Robo-Fc production by the transfection cells, in each experiment clusters of transfected cells were also embedded in collagen gels and cultured for 24 -72 hrs and fixed and stained with anti-human polyvalent immunoglobulins which bind to the Fc domain of the Robo2-Fc protein (Figure 6A). No Robo2-Fc protein was detected in cells transfected with the vector alone at any time point (Figure 6A), but was localised to clusters of cultured *Robo2-Fc* transfected cells from 0 hrs in vitro (48 hrs after transfection) until at least 72 hrs in vitro (the latest time point analysed; Figure 6A).

After grafting at HH St21 (~E3.5), limbs were left to develop to E7. Cartilage stains showed normal limb patterning in grafted limbs, with all cartilage elements present (Figure 6B). However, in limbs grafted with *Robo2-Fc* transfected cells the humerus was shorter compared to the contralateral unoperated limb (Figure 6B arrowhead, C, D). The ratio of the humerus length in grafted compared to the contralateral unoperated limb was 0.87 ± 0.01 for limbs grafted with *Robo2*-Fc expressing cells compared to 1.00 ± 0.02 for limbs grafted with control cells ($p < 0.01$; Student's unpaired t-test; Fig 6C). No significant difference was found in the relative length of the radius, ulna and digits 1-3 for limbs grafted with control or *Robo2-Fc* transfected cells (Figure 6B, C). Plotting the data using

estimation graphics, which illustrate effect sizes and their uncertainty,[45,46] confirmed that the relative length of the humerus, but not other limb elements, was shorter in *Robo2-Fc* grafted limbs (Fig 6D). This specific reduction in humerus length correlates with the proximo-central position of the grafted *Robo2-Fc* transfected cells, a region which fate maps have demonstrated gives rise to the humerus.[44]

Joint and tissue development appears normal in Robo2-Fc grafted chicken limbs

To determine if other aspects of limb development in addition to the length of the humerus were affected in *Robo2-Fc* grafted limbs, whole mount in situ hybridisation was performed for markers of joint patterning (*GDF5*), connective tissue (*SCX*), muscle (*MYOD1*) and blood vessels (*CDH5*). Limbs were examined 24hr and 48hr post-graft. At 48 hours post-graft *GDF5* expression was observed in two regions at the proximal mesenchyme, continuing as one band of expression distally to the hand-plate where a larger region was seen anteriorly and a smaller region of expression posteriorly in both Robo2-Fc grafted and contralateral limbs (Figure 7a, b). At HH St27, 48 hrs after grafting, connective tissue has yet to develop extensive patterning and *SCX* was expressed weakly at regions of metacarpal development in Robo2-Fc grafted and contralateral limbs (Figure 7c, d). *MYOD1* was widely expressed in the proximal limb mesenchyme, where expression continued distally to the handplate with weaker expression observed medially through the limb mesenchyme in Robo2-Fc grafted and contralateral limbs 24 hours post-graft (Figure 7e, f). At 48 hours post-graft in Robo2-Fc grafted and contralateral limbs, *MYOD1* was expressed in two large regions of proximal mesenchyme, continuing as two narrower lines of expression extending distally along anterior and posterior mesenchyme joining to form a thick region of expression in medial mesenchyme with no expression in the most distal mesenchyme (Figure 7g, h).

Defects in blood vessel development can also influence bone development.[47,48] For example, in *Vegfa*$^{120/120}$ mice, which express only the $VEGFA_{120}$ isoform, lengths of long bones are reduced.[49,50]

It is unclear whether Slit/Robo signalling acts as an attractant or repellent to endothelial cell migration,[19,51,52] however functioning as an attractant to endothelial cell growth during bone development would explain reduced limb cartilage elements upon neutralisation of Slit signalling. However, vascular networks appeared normal in Robo2-Fc grafted chicken limbs, at least at the time points analysed. At 24 hours post-graft, *CDH5* was expressed in capillary networks throughout the limb, with strongest expression observed at a single axial artery in Robo2-Fc grafted and contralateral limbs (Figure 7i, j). At 48 hours post-graft, *CDH5* was expressed in capillaries throughout the limb, more strongly expressed at the main axial artery plexus and in vascular rich regions between metacarpals, and absent from the cartilage condensations in Robo2-Fc grafted and contralateral limbs (Figure 7k, l). These findings demonstrate that joint, muscle, tendon and blood vessel development appear normal in *Robo2-Fc* grafted limbs, at least at early stages post-graft.

Cell death is not elevated in *Robo2-Fc* grafted chicken limbs

We used lysotracker red assay to determine if inhibition of Slit signalling through expression of Robo2-Fc altered cell death. Lysotracker is a dye that is rapidly taken up by lysosomes, and an increase in activity of lysosomes is correlated with increased cell death.[53] Lysotracker was used on limbs fixed 6hr and 24hr post graft (Figure 6A). In contralateral limbs and limbs grafted with control or Robo2-Fc transfected cells 6hr after grafting, lysotracker labelled an area of central, proximal mesenchyme at the cut site, as well as what appeared to be individual cells in a random fashion throughout the limb bud (Figure 8A arrowheads). Grafted cells were also labelled with lysotracker (Figure 8A, arrow). At 24hr post-graft, lysotracker labelled grafted cells in all grafted and contralateral limbs (Figure 8B arrowheads). We also noticed that lysotracker also detected the anterior necrotic zones of grafted and contralateral limbs, and which appeared unchanged in any of the limbs (Figure 8B arrows). Apart from labelling of cell aggregates, lysotracker did not identify areas of increased cell

death following grafting. We conclude that blocking Slit signalling does not elevate cell death in the developing limb.

Together, these results demonstrate that a local reduction in Slit-dependent signalling in the proximo-central region of the developing chicken limb reduces the length of the humerus but, at least in the first 24-48 hours following knockdown of signalling, does not impact on joint development, tissue patterning or cell death.

Discussion

Previous studies have described expression patterns of *Slits* and *Robos* in early mouse embryos. *Slit2* is expressed in the distal limb regions in the presumptive hand/footplate at E11.5 and *Slit3* in the proximal posterior region and distal anterior mesenchyme. At E12.5 *Slit2* is strongly expressed in interdigital regions, and expression fades as apoptosis takes place to separate digits.[2,9] No expression of *Slit1* was described during mouse limb development by Yuan et al. 1999[9] but was described at E12.5 in posterior and anterior margins and at the digit tips and over the joints at E13.5 by Holmes et al. 1998.[2] *Robo1* and *Robo2* are detected in proximal and central mesenchyme, respectively, at E11.5.[9,27] At E15.5 *Robo1* is expressed at regions along the digits resembling presumptive joint sites, suggesting a possible role in joint development, *Robo2* is expressed at digit tips and proximal digit regions and *Robo3* is not expressed during limb development (Table 1).[27]

In this paper, expression analysis of *Slits* and *Robos* during mouse fore- and hind-limb development demonstrated no expression of *Slit1*, in apparent conflict with Holmes et al. 1998.[2] A comparison of sequencing results reveals different nomenclature systems were implemented by Holmes et al. 1998[2] and Itoh et al. 1998[4] when vertebrate Slits were originally cloned: *Slit1* described by Holmes et al. 1998 refers to the *Slit3* described by Itoh et al. 1998 and Yuan et al. 1999.[2,4,9] The current official nomenclature of the mouse *Slit* genes follows the naming system adopted by Itoh et

al. 1998.[4] Consequently, the current official name for the mouse *Slit1* gene described in Holmes et al. 1998[2] is *Slit3*. Our findings therefore are in agreement with both Holmes et al, 1998[2] and Yuan et al, 1999,[9] demonstrating strong expression of *Slit2* and *Slit3*, but not *Slit1*, in the developing mouse limb.

Phenotypically normal *Slit1*$^{-/-}$, *Slit2*$^{-/-}$ compound mutants and *Slit3*$^{-/-}$ single mutant mouse limbs may be due to functional redundancy between Slits. Defects seen in *Slit* mutants are more profound when more than one *Slit* or *Robo* allele is disrupted, and often multiple genes are required to be lost before a phenotype is seen. For example, commissural axon guidance defects are see at the floorplate only in triple *Slit1*$^{-/-}$*Slit2*$^{-/-}$*Slit3*$^{-/-}$ mice.[36] Although subtle axon guidance defects are seen in single *Slit1*$^{-/-}$ and *Slit2*$^{-/-}$ mutants at the optic chiasm, defects are substantially more severe in *Slit1*$^{-/-}$*Slit2*$^{-/-}$ mice.[30] Moreover, previous studies have demonstrated that functional redundancy between Slits also can occur despite distinct expression patterns. For example, at the optic chiasm severe axon guidance defects are only observed in double *Slit1/2* mutant mice despite complementary, non-overlapping expression of *Slit1* and *Slit2* in the ventral diencephalon.[30,41,42] This could also be the case during mouse limb development, where at E14.5 and E15.5 *Slit2* is expressed interdigitally and *Slit3* in adjacent regions of proximal digit borders.

Following grafting of *Robo2-Fc* transfected cells into the proximo-central region of the developing chicken limb the length of the humerus but not other limb elements was affected. The most parsimonious explanation for the specific effect on the humerus is that it reflects the site at which the cells were grafted into the HH St21 forelimb bud combined with limited diffusion within the tissue of the Robo2-Fc generated by the transfected cells (Figure 8C). From DiI labelling fate maps cells in the proximo-central part of the developing limb remain where they are and end up in the humerus and elbow region.[44] Thus, influence of Robo2-Fc will likely be localised to the developing humerus. Unfortunately attempts to determine the extent of Robo2-Fc diffusion within the limb bud were not successful. Nevertheless, our results are consistent with a relatively local site of action. Future experiments using methods that enable more widespread expression of *Robo2-Fc* within the

developing limb will be required to determine if inhibiting Slit signalling throughout the limb bud affects the development of other limb cartilage elements. However, the Robo2-Fc construct is too large to insert into the RCAS viral vector commonly used for driving gene expression in chicken embryos.

A decrease in the length of the humerus could result from increased cell death, and/or an effect on bone, blood vessel, and/or neural development. However, lysotracker staining showed no change in cell death patterns in the limb. It is unclear whether *Robo1* or *Robo2* are expressed in chondrocytes. However, *Slit2* is reported to be expressed in periosteal cells and *Slit3* in both periosteal cells and proliferating chondrocytes in HH St30 chicken hindlimb.[26] *Slit2, Robo1* and *Robo2* are expressed during differentiation of rat osteoblasts *in vitro* and Slit2 acts as an inhibitor to osteoblast differentiation.[54] Slit3 is secreted by osteoclasts, promotes osteoblast migration and suppresses osteoclast differentiation.[55,56] Only deletion of osteoclast-specific *Slit3*, as opposed to osteoblast- or neuron-specific deletion, resulted in a reduction in bone mass.[56] Blood vessel development also appeared normal in limbs grafted with *Robo2-Fc* transfected cells. Further experiments therefore will be required to determine the mechanisms by which inhibiting Slit-signalling decreases the length of the humerus.

In conclusion, our functional experiments have demonstrated a role for Slit-Robo signalling in determining bone length, supporting a role for Slit-Robo signalling in bone development and/or homeostasis. Furthermore, a role for Slit-Robo signalling in joint homeostasis is supported by our expression pattern data showing *Slit3, Robo1* and *Robo2* in developing joint regions.

Experimental Procedures

Animals

All experimental procedures and conditions were in accordance with Institutional and the UK Animals (Scientific procedures) Act 1986 and associated Home Office guidelines. Fertilised White Leghorn chicken eggs were purchased from Henry Stewart, Norfolk, UK and incubated at 37°C to the desired developmental timepoint and staged according to Hamburger and Hamilton (1951).[57] The following mouse strains were used: C57BL/6J wild-type mice, *Slit1* and *Slit2* single and compound mutants on a mixed C57/BL/6J;129/Sv background and *Slit3* mutant mice on a C57BL/6J background.[29,30,58] Mice were mated and noon on the day of cervical plug formation counted as E0.5. Pregnant mothers were killed by cervical dislocation and the embryos either fixed in 4% formaldehyde in PBS (PFA) or tissue dissected and used for culture experiments or processed immediately for RNA extraction. Genotyping protocols are available on request.

Generation of riboprobes

To generate riboprobes for *mSlit3* and *cGDF5* RNA was extracted from embryonic tissues using the Qiagen RNeasy Kit and cDNA synthesised using SuperScript II (ThermoFisher Scientific) following the manufacturers' instructions. DNA fragments were amplified by PCR (94˚C for 5 min, 35 cycles of 94˚C for 40s, 55˚C for 1 min, 72˚C for 90 s followed by a final extension at 72˚C) and ligated into either pGEM T-Easy (Promega; *mSlit3*) or pBlueScript KS(+) (*cGDF5*). For *mSlit3* a 1:1 mixture of E14.5 and E15.5 mouse limb cDNA was used in the PCR, for *cGDF5* a 1:1 mixture of HH St20 (E3) and HH St25 (E5) chicken cDNA was used. The following primers were used: *mSlit3* F: AGCGAAAACCAGATCCAGGG R: TGGCAGTCGCAAACAAATGG; *cGDF5* F: GGTGACTCCAAAGGTCCCAA R: CAGTCCTGAGATCAACCGCT. The ligated plasmids were sequenced (DNA Sequencing and Services, University of Dundee) to confirm the identity and orientation of the inserted DNA. Other probes used were: mouse *Cdh5, Gdf5, Myod1*[32]*; Robo1, Robo2, Robo3, Slit1, Slit2* (Dr Tessier-Lavigne, The Rockefeller University)[1,41]; Scx[59] and chicken *SCX* (Dr Ronen Schweitzer, Oregon Health & Science University)[60]; *MYOD1* (Prof Ed Laufer, Columbia University)[61]; *CDH5* (Dr Jaffredo, Sorbonne University)[62]. Identity of all probe templates was

confirmed using sequencing (Table 2). In vitro transcription using DIG-labelled nucleotides (Sigma Aldrich) was used to generate antisense riboprobes.

Whole mount *in situ* hybridisation

Whole mount in situ hybridisation was performed on mouse and chicken embryos as described previously.[27] Briefly, embryos were fixed overnight in 4% PFA and dehydrated in three washes each of 50% and 100% methanol in PBT (PBS + 0.1% Tween-20) before bleaching in 6% H_2O_2 (Sigma Aldrich) in PBT, rehydration washes in 75%, 50% and 25% methanol in PBT and treatment with Proteinase K for 15 minutes (20mg/ml for mouse E13.5, E14.5 and chicken HH St 20-30; 30mg/ml for chicken HH St 30+; 40mg/ml for mouse E15.5). Embryos were post fixed in 4% PFA, washed in hybridisation solution (50% formamide, 5x SSC pH 4.5, 50µg/ml Heparin, 50µg/ml tRNA, 1% SDS) and incubated with required probe diluted 1:100 in hybridisation solution overnight at 65°C. The embryos were washed 3 times with Solution 1 (50% formamide, 5x SSC pH 4.5, 1% SDS) at 65˚C, 3 times with Solution 3 (50% formamide, 5x SSC pH 4.5) at 60˚C, followed by 3 washes with TBST (TBS + 1% Tween-20). The embryos were incubated for 60 min in 10% sheep serum in TBST before overnight incubation in anti-DIG-AP Fab fragments (Sigma Aldrich 11093274910; 1:5000 in 1% sheep serum in TBST). The embryos were washed for 24 hours in TBST before washes in NTMT (to make 100ml: 2ml 5M NaCl + 10ml 1M Tris-HCl (pH 9.5) + 5ml 1M $MgCl_2$ + 1ml Tween-20 + 82ml H_2O) and incubation at room temperature in colour solution (NTMT + BCIP (50mg/ml; 3.5µl per 1ml NTMT) + NBT (75mg/ml; 4.5µl per 1ml NTMT)). Colour reaction was terminated by several washes in PBS. For each gene and time point, analyses were performed on a minimum of 4 embryos.

Anti-neurofilament staining

Whole mount antibody staining was performed on mouse embryos as described previously.[26,57] Briefly, tissue was fixed in 4% PFA overnight at 4°C, transferred to Dent's bleach (33.3% H_2O_2; 66.6% Dent's fix) for 24 hours, washed in methanol and fixed in Dent's fix (20% DMSO, 80% methanol) for 24 hours. The tissue was washed in PBS and placed in blocking buffer (75% PBS, 20% DMSO, 5% goat

serum) for 1 hour at room temperature before incubation with anti-neurofilament antibody (Millipore AB1987; 1:50 in blocking buffer) for 24 hours at 4°C. The tissue was washed several times in PBS before incubation with Cy3-conjugated goat anti-rabbit IgG (Jackson ImmunoResearch; 1:1000 in blocking buffer) overnight at 4°C. The tissue was washed several times in PBS followed by 100% methanol and imaged and cleared in benzoic acid benzyl benzoate (BABB). For each genotype and time point, analyses were performed on 2 embryos.

Transfection of 293T cells and formation of cell aggregates

293T cells were cultured in DMEM/10% foetal calf serum/penicillin/streptomycin to 70 % confluency in 60 mm plates and transfected with the empty vector or a plasmid encoding Robo2-Fc (gift Dr Marc Tessier-Lavigne; Rockefeller University)[1], or Slit2 fused at its C terminus with a myc-tag (gift Dr Marc Tessier-Lavigne; Rockefeller University)[1,41] using Lipofectamine 3000 (ThermoFisher Scientific) according to the manufacturer's instructions. After 24 hrs, the cells were detached from the plates using trypsin (ThermoFisher Scientific) and resuspended at a density of 25 cells/µl in fresh culture medium. To generate clusters composed of a 1:1 ratio of *Robo2-Fc*, *Slit2* or vector transfected cells, following resuspension, the cells were mixed such that the final volume contained 50% of each cell type at density of 25 cells/µl. Drops of cells (20 µl) were aliquoted onto the inside of a lid of a sterile 90mm dish, the lid replaced on the dish and cultured for 48 hours to form aggregates of ~500 cells.

Collagen gel cultures of cell aggregates

Collagen gel cultures were prepared as described previously.[41,63] A 1:1 mix of bovine dermis collagen (VWR 392-2502) and rat tail collagen (VWR 734-1097) was prepared, and 10x DMEM and 0.8M $NaHCO_3$ added (enough to make the mixture light pink). Collagen (20 µl) was added to the centre of each well of a 4-well plate (Nunc) and left to set for 20 minutes at 37°C before cell aggregates were pipetted on top and covered in 20 µl collagen. Cultured cell aggregates were fixed in 4% PFA at 0, 24, 48 and 72 hours in vitro before PBS washes and blocking for 90 minutes with 10% goat serum, 0.2% Triton X-100 in PBS at room temperature. Cultures were incubated with FITC conjugated anti-human

polyvalent immunoglobulins (Sigma F-6506; 1:200 in blocking buffer) overnight (to detect the Fc portion of the Robo2-Fc construct) or in anti-myc (Developmental Studies Hybridoma Bank 9E10; 1:9 in blocking buffer) followed by Cy3-conjugated goat anti-mouse IgG (Jackson immunoresearch 1:2000 in 1% goat serum/PBS; to detect myc-tagged Slit2 protein).

Retinal explant culture experiments

Peripheral retina from E14.5 wild-type C57BL/6J mice were cultured in a 1:1 mixture of bovine dermis collagen (VWR 392-2502) and rat tail collagen (VWR 734-1097) as described previously[41,63]. For analysis of the effect of Slit2 and Robo2-Fc on axon outgrowth, explants were cultured 100 – 300 µm from clusters of ~500 293T cells composed of control cells transfected with the vector alone or 1:1 mixtures of control cells and *Robo2-Fc* transfected cells, control cells and *Slit2* transfected cells or *Robo2-Fc* and *Slit2* transfected cells. For analysis of the effect of Robo2-Fc on co-cultures of retina and ventral diencephalon tissue, the collagen mixture used to form the bottom layer of the collagen gel was seeded with control or *Robo2-Fc* transfected cells (3000 cells/µl; 60 000 cells/well). Explants were dissected from the ventral midline of the diencephalon as described previously[43] and co-cultured 100 – 300 µm from retinal explants in the collagen/cell mixture. The culture medium was composed of DMEM/F12 containing penicillin/streptomycin and ITS supplement (Sigma Aldrich). After 24 hrs the cultures were fixed and stained with anti-neuron-specific β-tubulin (Sigma Aldrich T8660; 1:500 in 10% goat serum/0.2% triton/PBS) followed by Cy-3 conjugated goat anti-mouse IgG (Jackson Immunoresearch; 1:2000 in 1% goat serum/PBS). The cultures were photographed using a Nikon SMZ1500 microscope and DXM1200 camera and the area covered by the RGC axons quantified using Image J (https://imagej.net/Welcome) as described[41,63]. Briefly, the retinal explant body was deleted from the image, the image was thresholded and converted to binary mode and the number of black pixels corresponding to the retinal axons quantified. The area of each retinal explant also was measured to ensure that differences in explant size did not impact on the results. Data are the mean from 3 independent experiments.

Forelimb surgical grafting experiments

A small window was made in the eggshell and the membranes covering the embryo removed. The upper-facing forelimb of Hamburger and Hamilton (HH) Stage (St) 21 embryo (approximately day 3.5 of development) was cut in the middle of the limb bud in an anterior to posterior orientation using a surgical blade (Altomed A10136). Aggregates of control (vector-transfected) cells or *Robo2-Fc* transfected cells were grafted into the forelimb cut. Only embryos with a single, stably inserted cell aggregate were used in analysis. Embryos were fixed 6hr, 24hr or 48hr after manipulation for expression analyses or at E7 (~ 4 days after manipulation) for cartilage staining. The contralateral limb was left un-operated to serve as a control.

Cartilage staining

E7 embryos were removed from the egg and fixed in 5% TCA overnight. The following day embryos were placed in to 0.1% Alcian blue for 24 hours, followed by 1% acid ethanol for 24 hours. The embryos were dehydrated in 3 washes of 100% ethanol and cleared and imaged in methyl salicylate (Sigma Aldrich). Limb cartilage elements were measured in Image J (https://imagej.net/Welcome). Results are from 7 independent experiments.

Cell death analysis

Chick limbs were dissected from the embryo 6 hrs and 24 hrs after grafting and placed in 12 well plates containing 2ml PBS/well. Lysotracker red (ThermoFisher Scientific; 25 µl) was diluted in 2ml PBS, 1.5ml PBS removed from each well and 200µl diluted lysotracker added. The plate was incubated, in the dark, at 37°C for 30 minutes. Limbs were washed 5x in PBS and fixed overnight in 4% PFA at 4°C. Limbs were rinsed with PBS and dehydrated by washes in 25%, 50% and 100% methanol. Tissue was stored and imaged in 100% methanol. For each time point analyses were performed on a minimum of 2 embryos.

Imaging

Whole mount images were captured using a Nikon SMZ1500 microscope with Nikon DS-L1 camera, section images using a Zeiss Axiophot microscope with a Nikon DXM1200 camera and whole mount antibody stains and collagen gel culture images using a Nikon SMZ1500 and a Nikon DXM1200 camera.

Statistical analysis

For null hypothesis significance testing, a Shapiro-Wilk test was used to confirm the data was normally distributed. Comparison of retinal explants cultured with transfected cells or diencephalon tissue, and lengths of the limbs in *Slit3* mutant mice was made using ANOVA with TUKEY post-hoc comparison. For comparison of the lengths of cartilage elements in chicken embryo limbs grafted with control or *Robo2-Fc* an unpaired student's t-test was used. Estimation graphics were generated using DABEST (data-analysis with bootstrap coupled estimation; https://www.estimationstats.com).[45,46]

Acknowledgements

This project was funded by an EastBio BBSRC DTP PhD Studentship to AR. The authors thank past and present lab staff for helpful discussions.

Data accessibility

Data supporting the findings of this study are available within the article or are available from corresponding authors upon reasonable request.

Conflicts of Interest

Authors declare no conflicts of interest

References

1. Brose K, Bland KS, Wang KH, et al. Slit proteins bind Robo receptors and have an evolutionarily conserved role in repulsive axon guidance. *Cell*. Mar 19 1999;96(6):795-806. https://doi.org10.1016/s0092-8674(00)80590-5.
2. Holmes GP, Negus K, Burridge L, et al. Distinct but overlapping expression patterns of two vertebrate slit homologs implies functional roles in CNS development and organogenesis. *Mech Dev*. Dec 1998;79(1-2):57-72. https://doi.org10.1016/s0925-4773(98)00174-9.
3. Huminiecki L, Gorn M, Suchting S, Poulsom R, Bicknell R. Magic roundabout is a new member of the roundabout receptor family that is endothelial specific and expressed at sites of active angiogenesis. *Genomics*. Apr 2002;79(4):547-52. https://doi.org10.1006/geno.2002.6745.
4. Itoh A, Miyabayashi T, Ohno M, Sakano S. Cloning and expressions of three mammalian homologues of Drosophila slit suggest possible roles for Slit in the formation and maintenance of the nervous system. *Brain Res Mol Brain Res*. Nov 20 1998;62(2):175-86. https://doi.org10.1016/s0169-328x(98)00224-1.
5. Kidd T, Bland KS, Goodman CS. Slit is the midline repellent for the robo receptor in Drosophila. *Cell*. Mar 19 1999;96(6):785-94. https://doi.org10.1016/s0092-8674(00)80589-9.
6. Li HS, Chen JH, Wu W, et al. Vertebrate slit, a secreted ligand for the transmembrane protein roundabout, is a repellent for olfactory bulb axons. *Cell*. Mar 19 1999;96(6):807-18. https://doi.org10.1016/s0092-8674(00)80591-7.
7. Nakayama M, Nakajima D, Nagase T, Nomura N, Seki N, Ohara O. Identification of high-molecular-weight proteins with multiple EGF-like motifs by motif-trap screening. *Genomics*. Jul 1 1998;51(1):27-34. https://doi.org10.1006/geno.1998.5341.
8. Simpson JH, Kidd T, Bland KS, Goodman CS. Short-range and long-range guidance by slit and its Robo receptors. Robo and Robo2 play distinct roles in midline guidance. *Neuron*. Dec 2000;28(3):753-66. https://doi.org10.1016/s0896-6273(00)00151-3.
9. Yuan W, Zhou L, Chen JH, Wu JY, Rao Y, Ornitz DM. The mouse SLIT family: secreted ligands for ROBO expressed in patterns that suggest a role in morphogenesis and axon guidance. *Dev Biol*. Aug 15 1999;212(2):290-306. https://doi.org10.1006/dbio.1999.9371.
10. Ypsilanti AR, Zagar Y, Chédotal A. Moving away from the midline: new developments for Slit and Robo. *Development*. Jun 2010;137(12):1939-52. https://doi.org10.1242/dev.044511.
11. Greenberg JM, Thompson FY, Brooks SK, Shannon JM, Akeson AL. Slit and robo expression in the developing mouse lung. *Dev Dyn*. Jun 2004;230(2):350-60. https://doi.org10.1002/dvdy.20045.
12. Grieshammer U, Le M, Plump AS, Wang F, Tessier-Lavigne M, Martin GR. SLIT2-mediated ROBO2 signaling restricts kidney induction to a single site. *Dev Cell*. May 2004;6(5):709-17. https://doi.org10.1016/s1534-5807(04)00108-x.
13. Hwang DY, Kohl S, Fan X, et al. Mutations of the SLIT2-ROBO2 pathway genes SLIT2 and SRGAP1 confer risk for congenital anomalies of the kidney and urinary tract. *Hum Genet*. Aug 2015;134(8):905-16. https://doi.org10.1007/s00439-015-1570-5.
14. Macias H, Moran A, Samara Y, et al. SLIT/ROBO1 signaling suppresses mammary branching morphogenesis by limiting basal cell number. *Dev Cell*. Jun 14 2011;20(6):827-40. https://doi.org10.1016/j.devcel.2011.05.012.
15. Piper M, Georgas K, Yamada T, Little M. Expression of the vertebrate Slit gene family and their putative receptors, the Robo genes, in the developing murine kidney. *Mech Dev*. Jun 2000;94(1-2):213-7. https://doi.org10.1016/s0925-4773(00)00313-0.
16. Jones CA, London NR, Chen H, et al. Robo4 stabilizes the vascular network by inhibiting pathologic angiogenesis and endothelial hyperpermeability. *Nat Med*. Apr 2008;14(4):448-53. https://doi.org10.1038/nm1742.

17. Jones CA, Nishiya N, London NR, et al. Slit2-Robo4 signalling promotes vascular stability by blocking Arf6 activity. *Nat Cell Biol*. Nov 2009;11(11):1325-31. https://doi.org10.1038/ncb1976.
18. Rama N, Dubrac A, Mathivet T, et al. Slit2 signaling through Robo1 and Robo2 is required for retinal neovascularization. *Nat Med*. May 2015;21(5):483-91. https://doi.org10.1038/nm.3849.
19. Wang B, Xiao Y, Ding BB, et al. Induction of tumor angiogenesis by Slit-Robo signaling and inhibition of cancer growth by blocking Robo activity. *Cancer cell*. Jul 2003;4(1):19-29. https://doi.org10.1016/s1535-6108(03)00164-8.
20. Mommersteeg MT, Andrews WD, Ypsilanti AR, et al. Slit-roundabout signaling regulates the development of the cardiac systemic venous return and pericardium. *Circ Res*. Feb 1 2013;112(3):465-75. https://doi.org10.1161/circresaha.112.277426.
21. Kramer SG, Kidd T, Simpson JH, Goodman CS. Switching repulsion to attraction: changing responses to slit during transition in mesoderm migration. *Science*. Apr 27 2001;292(5517):737-40. https://doi.org10.1126/science.1058766.
22. Ordan E, Volk T. A non-signaling role of Robo2 in tendons is essential for Slit processing and muscle patterning. *Development*. Oct 15 2015;142(20):3512-8. https://doi.org10.1242/dev.128157.
23. Ordan E, Volk T. Cleaved Slit directs embryonic muscles. *Fly*. 2015;9(2):82-5. https://doi.org10.1080/19336934.2015.1102808.
24. Wayburn B, Volk T. LRT, a tendon-specific leucine-rich repeat protein, promotes muscle-tendon targeting through its interaction with Robo. *Development*. Nov 2009;136(21):3607-15. https://doi.org10.1242/dev.040329.
25. Dickinson RE, Fegan KS, Ren X, Hillier SG, Duncan WC. Glucocorticoid regulation of SLIT/ROBO tumour suppressor genes in the ovarian surface epithelium and ovarian cancer cells. *PLoS One*. 2011;6(11):e27792. https://doi.org10.1371/journal.pone.0027792.
26. Holmes G, Niswander L. Expression of slit-2 and slit-3 during chick development. *Dev Dyn*. Oct 2001;222(2):301-7. https://doi.org10.1002/dvdy.1182.
27. Vargesson N, Luria V, Messina I, Erskine L, Laufer E. Expression patterns of Slit and Robo family members during vertebrate limb development. *Mech Dev*. Aug 2001;106(1-2):175-80. https://doi.orgS0925477301004300 [pii].
28. Denk AE, Kaufmann S, Stark K, et al. Slit3 inhibits Robo3-induced invasion of synovial fibroblasts in rheumatoid arthritis. *Arthritis research & therapy*. 2010;12(2):R45. https://doi.org10.1186/ar2955.
29. Dun XP, Carr L, Woodley PK, et al. Macrophage-Derived Slit3 Controls Cell Migration and Axon Pathfinding in the Peripheral Nerve Bridge. *Cell Rep*. Feb 5 2019;26(6):1458-1472.e4. https://doi.org10.1016/j.celrep.2018.12.081.
30. Plump AS, Erskine L, Sabatier C, et al. Slit1 and Slit2 cooperate to prevent premature midline crossing of retinal axons in the mouse visual system. *Neuron*. Jan 17 2002;33(2):219-32. https://doi.orgS0896627301005864 [pii].
31. Martin P. Tissue patterning in the developing mouse limb. *Int J Dev Biol*. Sep 1990;34(3):323-36.
32. Rafipay A, Berg ALR, Erskine L, Vargesson N. Expression analysis of limb element markers during mouse embryonic development. *Dev Dyn*. Nov 2018;247(11):1217-1226. https://doi.org10.1002/dvdy.24671.
33. Burton PR, Clayton DG, Cardon LR, et al. Genome-wide association study of 14,000 cases of seven common diseases and 3,000 shared controls. *Nature*. 2007/06/01 2007;447(7145):661-678. https://doi.org10.1038/nature05911.
34. Sharma S, Gao X, Londono D, et al. Genome-wide association studies of adolescent idiopathic scoliosis suggest candidate susceptibility genes. *Hum Mol Genet*. Apr 1 2011;20(7):1456-66. https://doi.org10.1093/hmg/ddq571.

35. Andrews W, Barber M, Hernadez-Miranda LR, et al. The role of Slit-Robo signaling in the generation, migration and morphological differentiation of cortical interneurons. *Dev Biol*. Jan 15 2008;313(2):648-58. https://doi.orgS0012-1606(07)01510-2 [pii]
10.1016/j.ydbio.2007.10.052.
36. Long H, Sabatier C, Ma L, et al. Conserved roles for Slit and Robo proteins in midline commissural axon guidance. *Neuron*. Apr 22 2004;42(2):213-23. https://doi.orgS0896627304001795 [pii].
37. Mommersteeg MT, Yeh ML, Parnavelas JG, Andrews WD. Disrupted Slit-Robo signalling results in membranous ventricular septum defects and bicuspid aortic valves. *Cardiovasc Res*. Apr 1 2015;106(1):55-66. https://doi.org10.1093/cvr/cvv040.
38. Liu J, Zhang L, Wang D, et al. Congenital diaphragmatic hernia, kidney agenesis and cardiac defects associated with Slit3-deficiency in mice. *Mech Dev*. Sep 2003;120(9):1059-70. https://doi.org10.1016/s0925-4773(03)00161-8.
39. Whitford KL, Marillat V, Stein E, et al. Regulation of cortical dendrite development by Slit-Robo interactions. *Neuron*. Jan 3 2002;33(1):47-61. https://doi.org10.1016/s0896-6273(01)00566-9.
40. Wu W, Wong K, Chen J, et al. Directional guidance of neuronal migration in the olfactory system by the protein Slit. *Nature*. Jul 22 1999;400(6742):331-6. https://doi.org10.1038/22477.
41. Erskine L, Williams SE, Brose K, et al. Retinal ganglion cell axon guidance in the mouse optic chiasm: expression and function of robos and slits. *J Neurosci*. Jul 1 2000;20(13):4975-82. https://doi.org20/13/4975 [pii].
42. Niclou SP, Jia L, Raper JA. Slit2 is a repellent for retinal ganglion cell axons. *J Neurosci*. Jul 1 2000;20(13):4962-74.
43. Wang LC, Rachel RA, Marcus RC, Mason CA. Chemosuppression of retinal axon growth by the mouse optic chiasm. *Neuron*. Nov 1996;17(5):849-62. https://doi.orgS0896-6273(00)80217-2 [pii].
44. Vargesson N, Clarke JD, Vincent K, Coles C, Wolpert L, Tickle C. Cell fate in the chick limb bud and relationship to gene expression. *Development*. May 1997;124(10):1909-18.
45. Calin-Jageman RJ, Cumming G. Estimation for Better Inference in Neuroscience. *eNeuro*. Jul-Aug 2019;6(4). https://doi.org10.1523/eneuro.0205-19.2019.
46. Ho J, Tumkaya T, Aryal S, Choi H, Claridge-Chang A. Moving beyond P values: data analysis with estimation graphics. *Nature methods*. Jul 2019;16(7):565-566. https://doi.org10.1038/s41592-019-0470-3.
47. Mende K, Vargesson N, Sivakumar B. Vascular anomalies of the upper limb. *J Hand Surg Eur Vol*. Mar 2019;44(3):233-241. https://doi.org10.1177/1753193418808130.
48. Vargesson N, Hootnick DR. Arterial dysgenesis and limb defects: Clinical and experimental examples. *Reproductive toxicology*. Jun 2017;70:21-29. https://doi.org10.1016/j.reprotox.2016.10.005.
49. Gerber HP, Vu TH, Ryan AM, Kowalski J, Werb Z, Ferrara N. VEGF couples hypertrophic cartilage remodeling, ossification and angiogenesis during endochondral bone formation. *Nat Med*. Jun 1999;5(6):623-8. https://doi.org10.1038/9467.
50. Maes C, Carmeliet P, Moermans K, et al. Impaired angiogenesis and endochondral bone formation in mice lacking the vascular endothelial growth factor isoforms VEGF164 and VEGF188. *Mech Dev*. Feb 2002;111(1-2):61-73. https://doi.org10.1016/s0925-4773(01)00601-3.
51. Fujiwara M, Ghazizadeh M, Kawanami O. Potential role of the Slit/Robo signal pathway in angiogenesis. *Vascular medicine (London, England)*. May 2006;11(2):115-21. https://doi.org10.1191/1358863x06vm658ra.
52. Park KW, Morrison CM, Sorensen LK, et al. Robo4 is a vascular-specific receptor that inhibits endothelial migration. *Dev Biol*. Sep 01 2003;261(1):251-67.

53. Fogel JL, Thein TZ, Mariani FV. Use of LysoTracker to detect programmed cell death in embryos and differentiating embryonic stem cells. *J Vis Exp*. Oct 11 2012;(68). https://doi.org10.3791/4254.
54. Sun H, Dai K, Tang T, Zhang X. Regulation of osteoblast differentiation by slit2 in osteoblastic cells. *Cells, tissues, organs*. 2009;190(2):69-80. https://doi.org10.1159/000178020.
55. Iqbal J, Yuen T, Kim SM, Zaidi M. Opening windows for bone remodeling through a SLIT. *J Clin Invest*. Apr 2 2018;128(4):1255-1257. https://doi.org10.1172/jci120325.
56. Kim BJ, Lee YS, Lee SY, et al. Osteoclast-secreted SLIT3 coordinates bone resorption and formation. *J Clin Invest*. Apr 2 2018;128(4):1429-1441. https://doi.org10.1172/jci91086.
57. Hamburger V, Hamilton HL. A series of normal stages in the development of the chick embryo. *J Morphol*. Jan 1951;88(1):49-92.
58. Yuan W, Rao Y, Babiuk RP, Greer JJ, Wu JY, Ornitz DM. A genetic model for a central (septum transversum) congenital diaphragmatic hernia in mice lacking Slit3. *Proc Natl Acad Sci U S A*. Apr 29 2003;100(9):5217-22. https://doi.org10.1073/pnas.0730709100.
59. Cserjesi P, Brown D, Ligon KL, et al. Scleraxis: a basic helix-loop-helix protein that prefigures skeletal formation during mouse embryogenesis. *Development*. Apr 1995;121(4):1099-110.
60. Schweitzer R, Chyung JH, Murtaugh LC, et al. Analysis of the tendon cell fate using Scleraxis, a specific marker for tendons and ligaments. *Development*. Oct 2001;128(19):3855-66.
61. Fujisawa-Sehara A, Nabeshima Y, Komiya T, Uetsuki T, Asakura A, Nabeshima Y. Differential trans-activation of muscle-specific regulatory elements including the mysosin light chain box by chicken MyoD, myogenin, and MRF4. *J Biol Chem*. May 15 1992;267(14):10031-8.
62. Bollerot K, Romero S, Dunon D, Jaffredo T. Core binding factor in the early avian embryo: cloning of Cbfbeta and combinatorial expression patterns with Runx1. *Gene Expr Patterns*. Dec 2005;6(1):29-39. https://doi.org10.1016/j.modgep.2005.05.003.
63. Erskine L, Reijntjes S, Pratt T, et al. VEGF signaling through neuropilin 1 guides commissural axon crossing at the optic chiasm. *Neuron*. Jun 9 2011;70(5):951-65.
64. Marillat V, Sabatier C, Failli V, et al. The slit receptor Rig-1/Robo3 controls midline crossing by hindbrain precerebellar neurons and axons. *Neuron*. Jul 8 2004;43(1):69-79. https://doi.org10.1016/j.neuron.2004.06.018.

Figure legends

Figure 1. Expression of *Slit1*, *Slit2*, *Slit3, Robo1, Robo2* and *Robo3* during mouse limb development.

(a-r') Whole-mount *in situ* hybridisation with probes specific for S*lit1* (a, a', g, g', m, m'), S*lit2* (b, b', h, h', n, n'), *Slit3* (c, c', i, i', o, o'), *Robo1* (d, d', j, j', p, p'), *Robo2* (e, e', k, k', q, q') and *Robo3* (f, f', l, l', r, r') at E13.5 (a-f'), E14.5 (g-l'), E15.5 (m-r') in forelimbs (FL) and hindlimbs (HL), dorsal view. (s-x) Transverse sections through E15.5 forelimb digits stained by whole-mount in situ hybridisation for *Slit1* (s), *Slit2* (t), *Slit3* (u), *Robo1* (v), *Robo2* (w) and *Robo3* (x). Arrowheads in (b, b', t) indicate expression of *Slit2* in interdigital mesenchyme, arrows in (i, i', o, o') indicate broader regions of *Slit3*

expression along digit borders prior to developing joint sites, arrowheads in (o, o') indicate *Slit3* expression in distal interphalangeal joints., arrowheads in (d, d') indicate *Robo1* expression in cartilage condensations, arrow in (d) indicates expression in the forelimb proximal interphalangeal joint, arrowheads in (p, p') indicate *Robo1* expression in developing joint regions, arrowhead in (e) indicates *Robo2* expression in forelimb chondrogenic condensations, arrows in (q, q', w) indicate *Robo2* expression around developing joints, and arrowheads in (q, q', w) indicate expression at the distal interphalangeal joint. FL: forelimb, HL: hindlimb. Scale bars, 500 µm.

Figure 2. Length and patterning of limb elements is normal in *Slit1/2* mutant mice. (A, B) Relative lengths of E15.5 *Slit1*$^{-/-}$ compared to *Slit1*$^{+/+}$ littermate and *Slit1*$^{-/-}$ *Slit2*$^{-/-}$ compared to *Slit1*$^{-/-}$ *Slit2*$^{+/+}$ littermate forelimbs (A) and hindlimbs (B). Numbers analysed: *Slit1*$^{-/-}$ n = 3; *Slit1*$^{+/+}$ n = 4; *Slit1*$^{-/-}$ *Slit2*$^{-/-}$ n = 5; *Slit1*$^{-/-}$ *Slit2*$^{+/+}$ n = 4. (C) Whole mount *in-situ* hybridisation for *Gdf5* and *Cdh5* in E15.5 forelimbs (FL), for *Scx* in E14.5 forelimbs and for *Myod1* in E15.5 hindlimbs (HL) of *Slit1*$^{+/+}$ and *Slit1*$^{-/-}$*Slit2*$^{-/-}$ mice, dorsal view. White arrows indicate *Gdf5* expression in proximal interphalangeal joints, black arrows *Cdh5* expression at developing interzones and black arrowheads *Scx* expression at developing proximal interphalangeal joints. Scale bars, 500µm.

Figure 3. Nerve patterning is normal in *Slit1/2* mutant mice. Anti-neurofilament staining of developing nerves in E11.5 forelimbs (FL; a-c) and hindlimbs (HL; a'-c'), E13.5 forelimbs (d-f) and E14.5 forelimbs (g-i) of *Slit1*$^{+/+}$ (a, a', d, g), *Slit1*$^{-/-}$ (b, b', e, h) and *Slit1*$^{-/-}$*Slit2*$^{-/-}$ (c, c', f, i) mice. White arrows indicate nerves entering the forelimbs at E11.5, white asterisks two main nerve branches entering the E11.5 hindlimbs, and white arrowheads distal development of nerves in E14.5 forelimbs. Scale bars, 500 µm.

Figure 4. *Slit3* mutant mouse limbs appear phenotypically normal. (A) Mean (± s. d.) hindlimb lengths of E15.5 *Slit3*$^{+/+}$, *Slit3*$^{+/-}$ and *Slit3*$^{-/-}$ mice. ns: not significant. ANOVA with TUKEY post-hoc comparison. Numbers on bars indicate numbers analysed. (B) Whole mount *in-situ* hybridisation for *Cdh5* and *Myod1* in E15.5 forelimbs (FL) of *Slit3*$^{+/+}$ and *Slit3*$^{-/-}$ mice. Scale bars, 500µm.

Figure 5. Robo2-Fc inhibits Slit signalling. (A) Representative examples of retinal explants co-cultured in collagen gels at a short distance (100 – 300 μm) from clusters of control 293T cells transfected with the vector alone or 1:1 mixtures of control and *Robo2-Fc* transfected cells, control and *Slit2* transfected cells or *Slit2* and *Robo2-Fc* transfected cells. The cultures were fixed after 24 hrs and stained with antibodies against neuron-specific β-tubulin to label the retinal ganglion cell axons. Inserts show representative examples of cell clusters stained with anti-human polyvalent immunoglobulins (green) to label the Robo2-Fc produced by the transfected cells and anti-myc (red) to label the myc-tagged Slit2 protein produced by the transfected cells. (B) Representative examples of retinal explants cultured in the presence and absence of ventral diencephalon (dienceph) tissue in collagen gels seeded with control 293T cells transfected with the vector alone or transfected with *Robo2-Fc.* The cultures were fixed after 24 hrs and stained with antibodies against neuron-specific β-tubulin to label the retinal ganglion cell axons. Inserts show representative examples of control and *Robo2-Fc* transfected 293T cells within the collagen gels stained with anti-human polyvalent immunoglobulins (green) to label the Robo2-Fc produced by the transfected cells. (C) Mean (± s.e.m.) area covered by the retinal ganglion cell axons from retinal explants cultured in the presence of clusters of control cells transfected with the vector alone or formed from 1:1 mixtures of control and *Robo2-Fc* transfected cells, control and *Slit2* transfected cells or *Slit2* and *Robo2-Fc* transfected cells. (D) Mean (± s.e.m.) area covered by RGC axons from retinal explants cultured in collagen gels seeded with control or *Robo2*-Fc transfected cells in the presence or absence of ventral diencephalon tissue. Numbers on bars indicate number of explants analysed. Data are from 3 independent experiments. ** = $p < 0.01$, * = $p < 0.05$; ANOVA with TUKEY post-hoc comparison. Scale bars, 200 μm.

Figure 6. Local suppression of Slit signalling in the proximo-central region of developing chicken limbs decreases the length of the humerus. (A) Representative examples of clusters of 293T cells transfected with the vector alone (control) or transfected with *Robo2-Fc* and fixed and stained with

antibodies against the Fc domain at 0hr (time of culturing in collagen; 48 hrs after transfection), 24hr, 48hr and 72hr after culturing in collagen. Scale bars, 200 µm. (B) Cartilage stains of contralateral control (unoperated) chicken limbs and limbs grafted at HH St21 (~E3.5) with clusters of control 293T cells transfected with the vector alone or transfected with *Robo2-Fc* and fixed at E7. White arrow, points to shortened humerus in limbs following graft of *Robo2-Fc* transfected cells. H, humerus, R, radius, U, ulna, D1, digit 1, D2, Digit2, D3, Digit3. Scale bars, 500 µm. (C) Mean (± s.e.m.) relative length of the humerus, radius, ulna, Digit 1, Digit 2 and Digit 3 of limbs grafted with clusters of control 293T cells transfected with the vector alone (white bars) or transfected with *Robo2-Fc* (grey bars) expressed as a ratio of the length in the contralateral (unoperated) limb. *** = $p < 0.001$ compared to limbs grafted with the control cells; Student's unpaired t-test. Numbers on bars indicate number of embryos analysed. (D) Cumming Estimation plots showing the mean difference for the relative length in of the humerus, radius, ulna, Digit 1, Digit 2, and Digit 3 for limbs grafted with control cells transfected with the vector alone or *Robo2-Fc* transfected cells. Data are expressed as the ratio of the limb element length in the grafted: contralateral unoperated limb. The raw data is plotted on the upper axes and each mean difference is plotted on the lower axes as a bootstrap sampling distribution. Mean differences are indicated on the lower plots by the dots and the 95% confidence intervals by the ends of the vertical error bars. The unpaired mean difference between the length of the humerus in limbs grafted with control versus *Robo2-Fc* transfected cells is 0.124 [95% CI -0.168 lower limit, -0.0938 upper limit]. The p value of the two-sided permutation t-test is 0.0. All other comparisons are not significant (radius, p = 0.109; ulna, p = 0.542 Digit 1, p = 0.899; Digit 2, p = 0.553; Digit 3, p = 0.315).

Figure 7. Skeletal and tissue elements appear normal in chicken limbs grafted with Robo2-Fc. (a-l) Whole mount *in situ* hybridisation for *GDF5* (a, b), *SCX* (c, d), *MYOD1* (e-h) and *CDH5* (i-l) 24hr (e, f, I, j) and 48hr (a-d, g, h, k, l) after grafting at HH St21 with *Robo2-Fc* transfected cells and in the contralateral control (unoperated) limb. Arrowheads in (a, b) indicate proximal regions of *GDF5* expression, arrows in (a, b) distal regions of *GDF5* expression, arrows in (c, d) *SCX* expression at regions of metacarpal development, arrows in (e, f) weak *MYOD1* expression in central mesenchyme, arrows

in (g, h) a single expression domain of *MYOD1* in distal mesenchyme, arrows in (I, j) strong expression of *CDH5* at the position of the axial artery. Scale bars, 500 µm.

Figure 8. Cell death is not elevated in grafted limbs. (A, B) Lysotracker red cell death staining on contralateral (unoperated) chicken embryo limbs and limbs 6hr (A) and 24hr (B) after grafting with clusters of control cells transfected with the vector alone or cells transfected with *Robo2-Fc*. Arrows in (A) and (B) indicate lysotracker labelling of grafted cells, arrowheads in (A) lysotracker labelling of proximal central mesenchyme, and arrowheads in (B) lysotracker labelling of anterior necrotic zones. Scale bars, 500µm. (C) schematic diagrams showing location of grafted cells immediately after grafting at HH St21 and 24 hours later.

Tables

Table 1. Comparisons of expression patterns of Slits and Robos during chicken and mouse embryo limb development.

Gene	Chicken Developmental Stage	Equivalent mouse developmental stage	Expression in chicken limbs*	Expression in mouse limbs
Slit1	HH St28	E13.5	Around digit tip	Not detected
Slit2	HH St28	E13.5	Peridigital	Interdigital
Slit3	HH St28	E13.5	Peridigital, distal mesenchyme	Proximal mesenchyme
Robo1	HH St28	E13.5	Distal mesenchyme, bordering AER	Developing joints
Robo1	HH St32	E14.5	Digit tips and digit border	Along each digit at sites of developing joints
Robo1	HH St36	E15.5	Digit tips, dominas along each digit at sites of developing joints	Along each digit at sites of developing joints
Robo2	HH St28	E13.5	Proximal peridigital mesenchyme	Proximal digit and peridigital mesenchyme
Robo2	HH St32	E14.5	Interdigital mesenchyme, digit borders	Proximal mesenchyme around sites of developing joints
Robo2	HH St36	E15.5	Peridigital, digit tips	Around developing joints, digit tips.
Robo3			Not detected	Not detected

* Data from [26,27].

Table 2 Sequences of Riboprobe Templates

Gene	Species	Sequence ID:	Nucleotides	Reference
Cdh5	Mouse	NM_009868.4	1671 – 2383	32
CDH5 (VE-Cadherin)	Chicken	XM_015292499.2	629 – 1679	62
Gdf5	Mouse	NM_008109.3	916 – 1748	32
GDF5	Chicken	NM_204338.1	354 – 976	This paper
Myod1	Mouse	NM_010866.2	324 – 805	32
Robo1	Rat* (mouse)	NM_022188.1 (NM_0194132.2)	173 – 1075 (938 – 1947; 92% identity)	1
Robo2	Rat* (mouse)	NM_032106.3 (NM_001358493.1)	<2095 – 3331 <1622 – 2858; 93% identity)+	1
Robo3 (Rig-1)	Mouse	AF060570.1	<4339 – 4580+	64
Scx	Mouse	NM_198885.3	188 – 999	59
SCX	Chicken	NM_204253.1	668 – 1133	60
Slit1	Rat* (mouse)	NM_022953.2 (NM_105748.3)	2515 – 3261 (2804 – 3550; 95% identity)	1
Slit2	Rat* (mouse)	NM_022632.2 (NM_001291227.2)	<3830 - 5109 <5247- 6515; 94% identity)+	1
Slit3	Mouse	NM_011412.3	480 - 1390	This paper

* *Robo1, Robo2, Slit1, Slit2* probe templates were cloned from rat. Sequences recognised in mouse and % identity of probes to these regions in mouse also are given.

+Sequences for *Robo2, Robo3* and *Robo3* riboprobe templates are longer than given in the table (*Robo2* ~1.7kb; *Slit2* ~ 1.6kb; *Robo3* ~1.2kb)

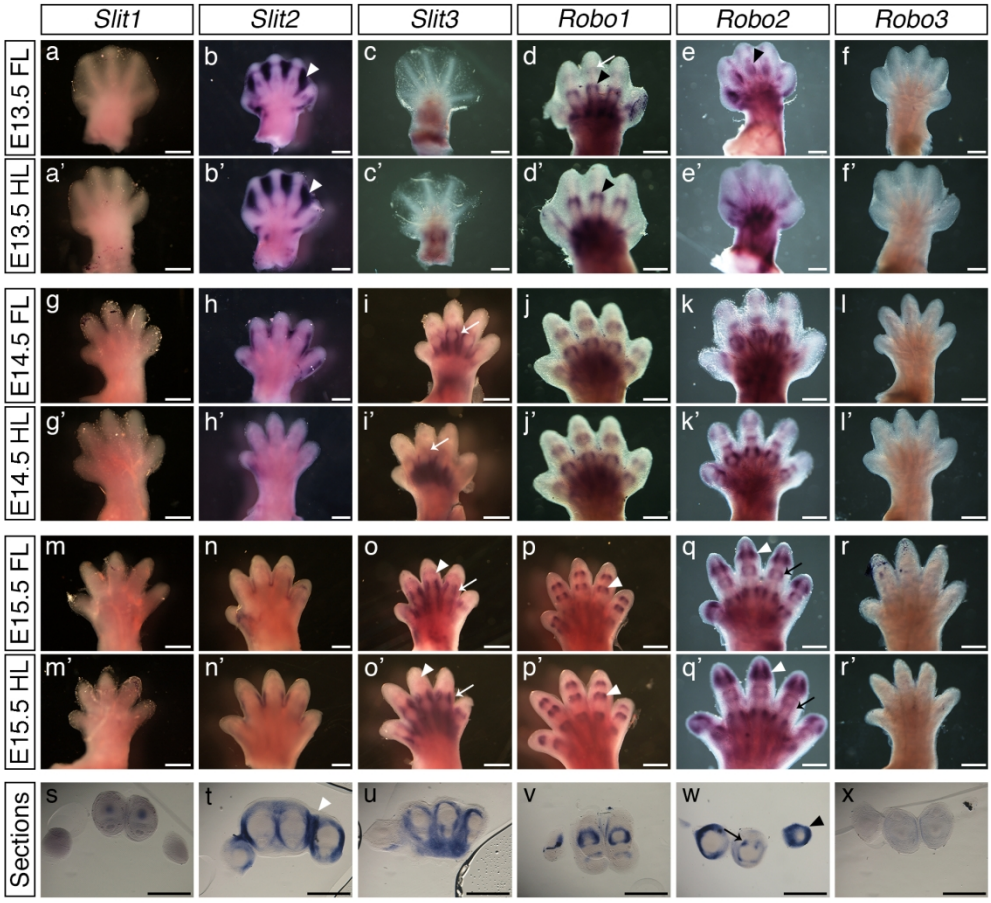
Slit1
Slit2
Slit3
Robo1
Robo2
Robo3
E13.5 FL
E13.5 HL
E14.5 FL
E14.5 HL
E15.5 FL
E15.5 HL
Sections

Figure 1


(A)
Forelimb Length
% of control
120
100
80
60
40
20
0
Slit1-/-
Slit1-/- Slit2-/-
(B)
Hindlimb Length
% of control
120
100
80
60
40
20
0
Slit1-/-
Slit1-/- Slit2-/-
(C)
Slit1+/+
Slit1-/- Slit2-/-
E15.5 FL Gdf5
E15.5 FL Cdh5
E14.5 FL Scx
E15.5 HL Myod1

Figure 2

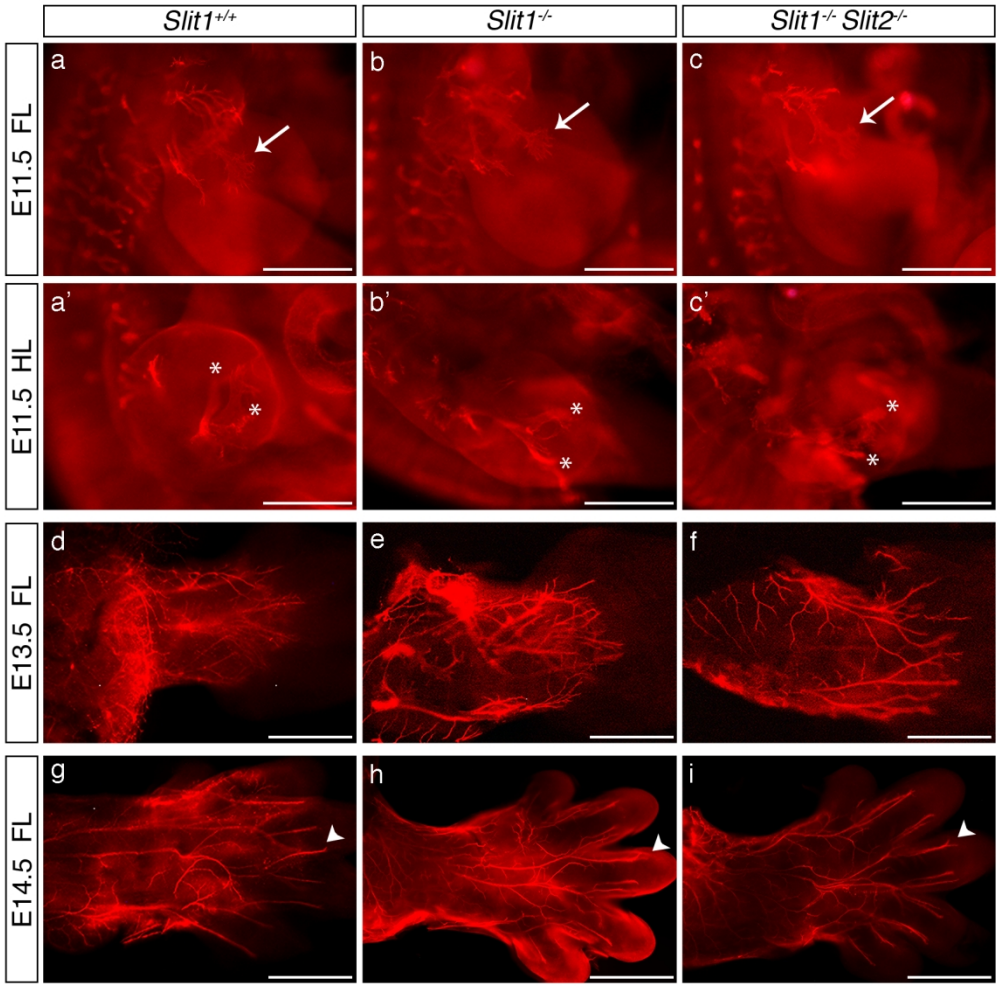
Slit1+/+
Slit1-/-
Slit1-/- Slit2-/-
E11.5 FL
E11.5 HL
E13.5 FL
E14.5 FL
a
b
c
a'
b'
c'
d
e
f
g
h
i

Figure 3

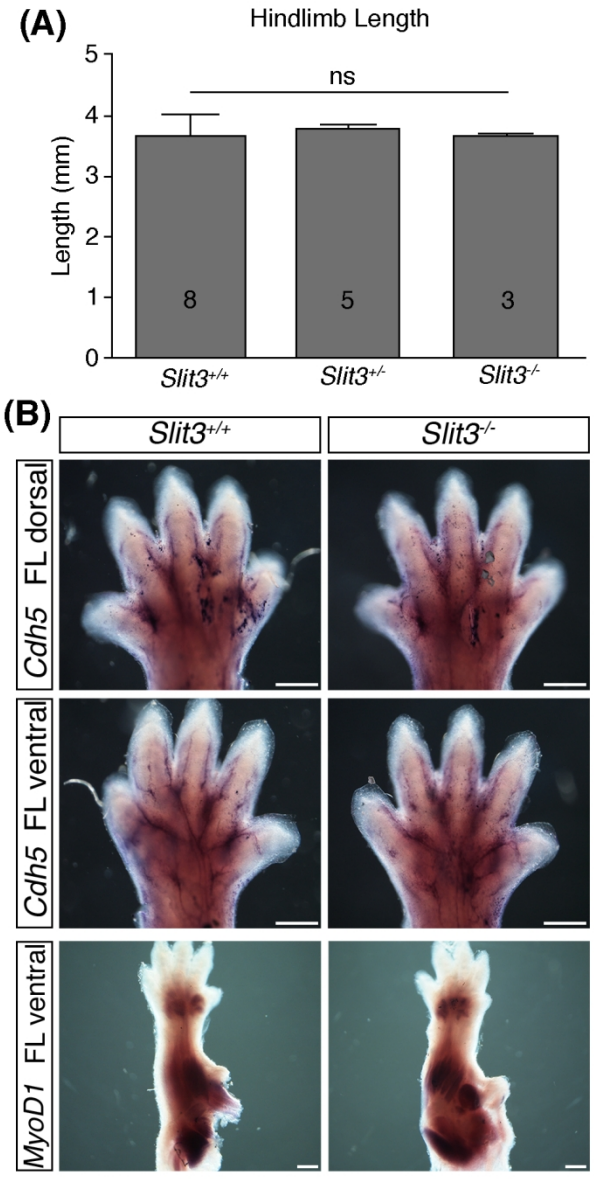
(A)
Hindlimb Length
ns
Length (mm)
0
1
2
3
4
5
8
5
3
Slit3+/+
Slit3+/-
Slit3-/-
(B)
Slit3+/+
Slit3-/-
Cdh5 FL dorsal
Cdh5 FL ventral
MyoD1 FL ventral

Figure 4

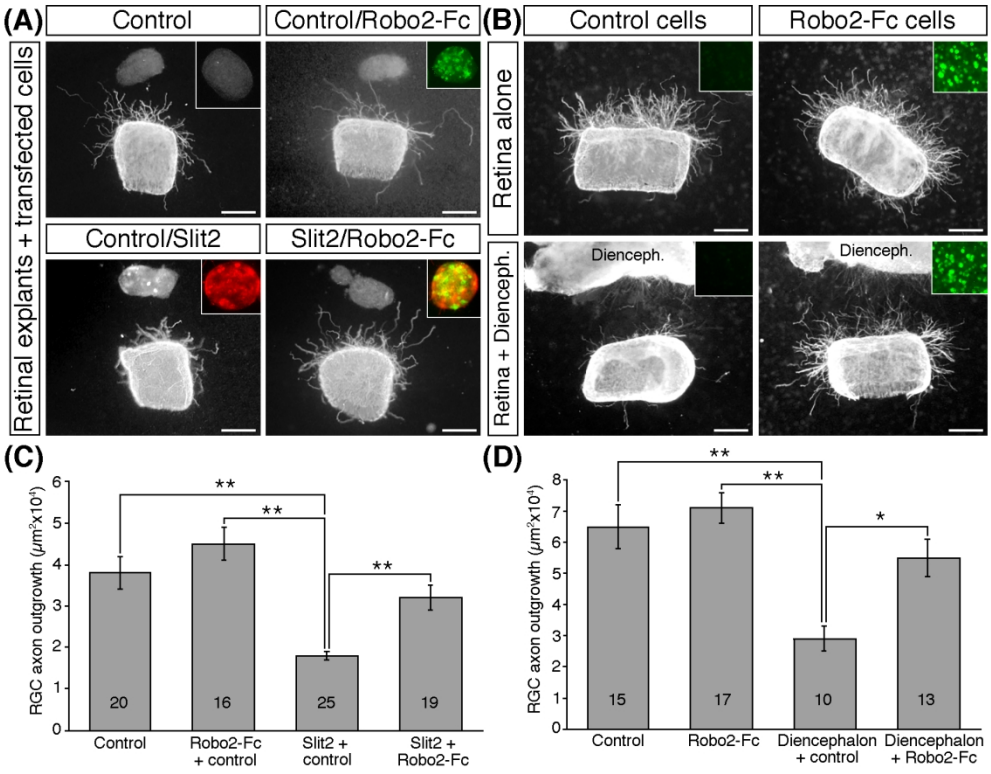
(A)
Control
Control/Robo2-Fc
Control/Slit2
Slit2/Robo2-Fc
Retinal explants + transfected cells
(B)
Control cells
Robo2-Fc cells
Retina alone
Retina + Dienceph.
Dienceph.
Dienceph.
(C)
RGC axon outgrowth (μm²x10⁴)
**
**
**
20
16
25
19
Control
Robo2-Fc + control
Slit2 + control
Slit2 + Robo2-Fc
(D)
RGC axon outgrowth (μm²x10⁴)
**
**
*
15
17
10
13
Control
Robo2-Fc
Diencephalon + control
Diencephalon + Robo2-Fc

Figure 5

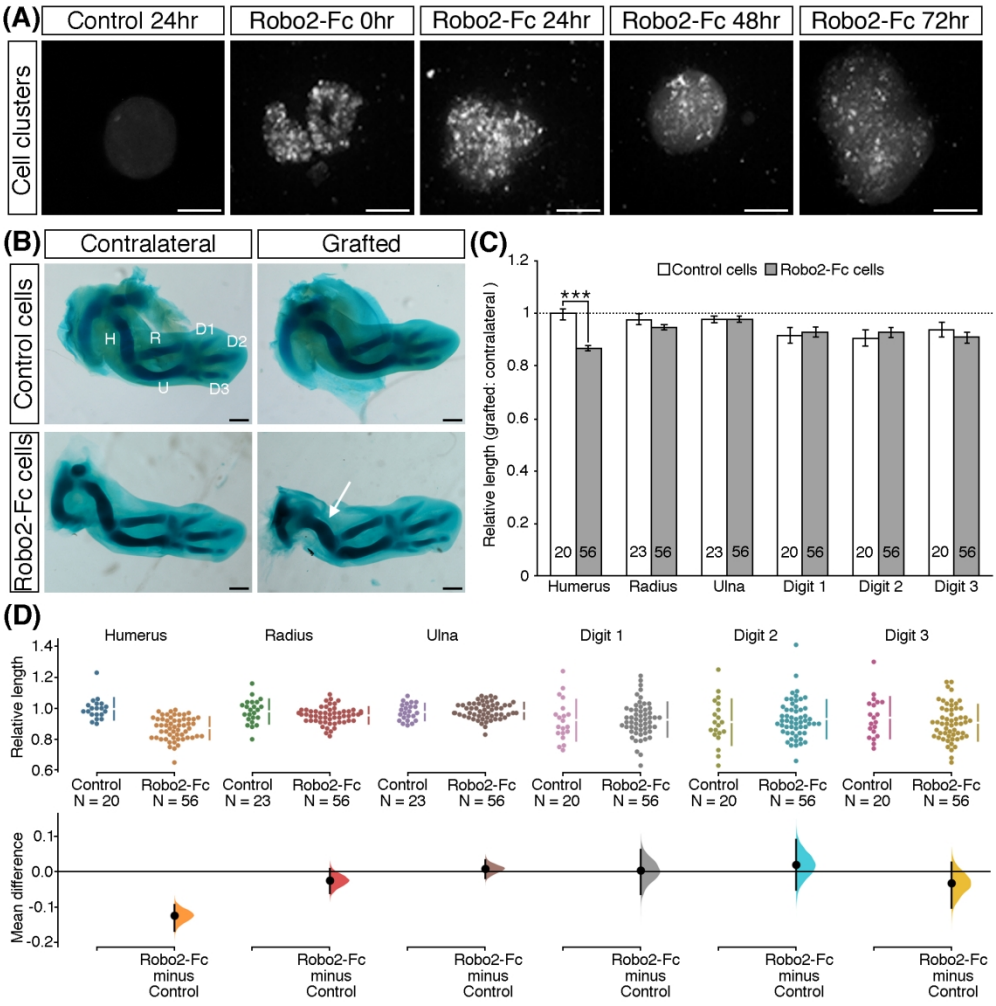
(A)
Control 24hr
Robo2-Fc 0hr
Robo2-Fc 24hr
Robo2-Fc 48hr
Robo2-Fc 72hr
Cell clusters
(B)
Contralateral
Grafted
Control cells
Robo2-Fc cells
H
R
D1
D2
U
D3
(C)
Control cells
Robo2-Fc cells
Relative length (grafted: contralateral)
***
Humerus
Radius
Ulna
Digit 1
Digit 2
Digit 3
(D)
Relative length
Mean difference
Control
Robo2-Fc
N = 20
N = 56
N = 23
Robo2-Fc minus Control

Figure 6

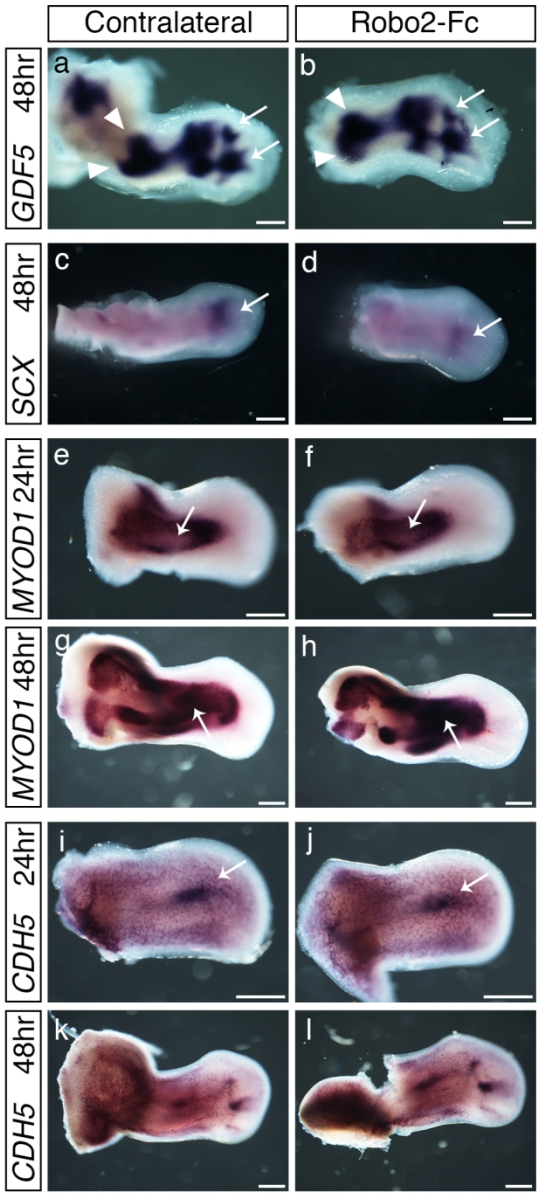
Contralateral
Robo2-Fc
GDF5 48hr
SCX 48hr
MYOD1 24hr
MYOD1 48hr
CDH5 24hr
CDH5 48hr
a
b
c
d
e
f
g
h
i
j
k
l

Figure 7

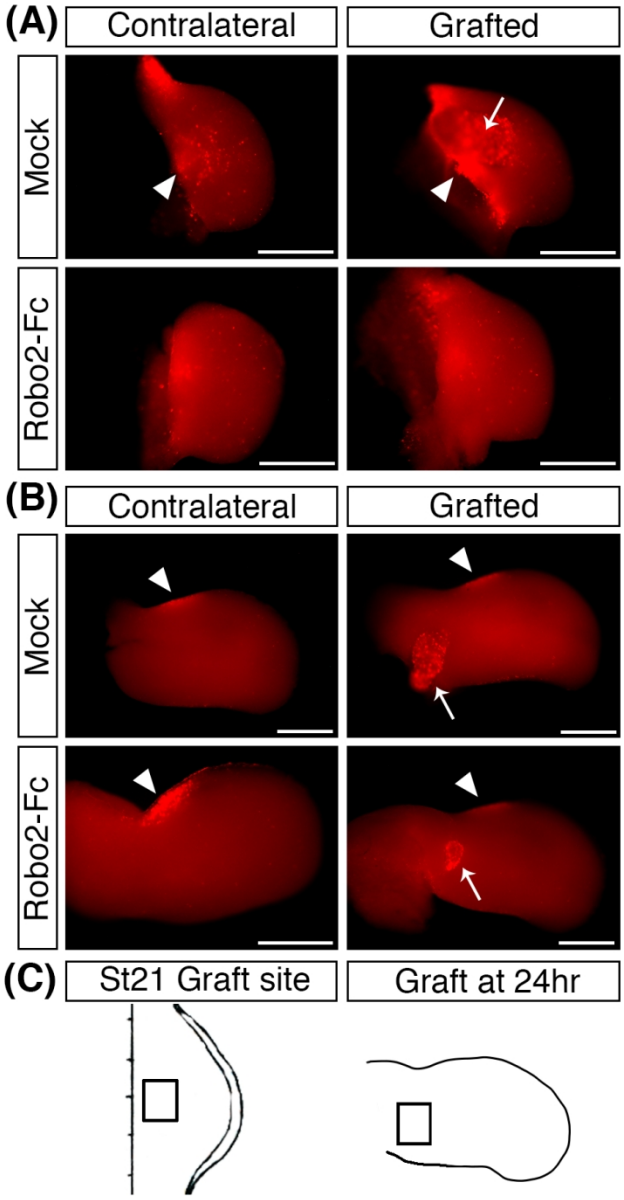
(A)
Contralateral
Grafted
Mock
Robo2-Fc
(B)
Contralateral
Grafted
Mock
Robo2-Fc
(C)
St21 Graft site
Graft at 24hr

Figure 8